

Article

A Novel Approach towards the Preparation of Silk-Fibroin-Modified Polyethylene Terephthalate with High Hydrophilicity and Stability

Jingyi Fan ^{1,2,3}, Yiwen Zhang ^{1,2,3}, Maoyang Li ^{1,2,3}, Peiyu Ji ^{1,2,3}, Haiyun Tan ^{1,2,3}, Tianyuan Huang ^{1,2,3}, Lanjian Zhuge ⁴, Xiaoman Zhang ^{1,2,3,*} and Xuemei Wu ^{1,2,3,*} 

- ¹ School of Physical Science and Technology, Soochow University, Suzhou 215123, China; jyfanfy@stu.suda.edu.cn (J.F.); 20214208031@stu.suda.edu.cn (Y.Z.); 17683703549@163.com (M.L.); pyji@suda.edu.cn (P.J.); hytan@suda.edu.cn (H.T.); tyhuang@suda.edu.cn (T.H.)
² Collaborative Innovation Center of Suzhou Nano Science and Technology, Soochow University, Suzhou 215123, China
³ The Key Laboratory of Thin Films of Jiangsu, Soochow University, Suzhou 215123, China
⁴ Analysis and Testing Center, Soochow University, Suzhou 215123, China; ljhuge@suda.edu.cn
* Correspondence: xmzhang23@suda.edu.cn (X.Z.); xmwu@suda.edu.cn (X.W.)

Abstract: Silk fibroin (SF) has been widely used in biomedical applications for the hydrophilicity modification of high molecular polymer materials. However, the challenge remains to immobilize SF with high structure stability and strong adhesion strength between SF and the substrate. Here, we propose an effective two-step process for modifying polyethylene terephthalate (PET) with SF: dipping PET film in SF solution and subsequently carrying out plasma-assisted deposition in SF aerosol. The structure and property analysis revealed that the SF-modified PET (PET-SF) prepared using the two-step method exhibited superior structural stability and stronger adhesion strength compared to the dip-coating method and the plasma-assisted deposition method. In addition, PET-SF prepared using the two-step method resulted in a higher concentration of SF and an increased content of active groups on its surface, enhancing its hydrophilicity compared to the other two methods. Additionally, the influence of dipping time and deposition time in the two-step method was investigated. The results demonstrated that the dipping time for 6 h and the deposition time for 3 min resulted in maximum SF grafting amount with a highly stable structure. Furthermore, the PET-SF exhibited satisfactory hydrophilicity when the deposition time was more than 3 min and showed the most hydrophilicity surface at 8 min.

Keywords: plasma-assisted deposition; solution dip-coating; silk fibroin



Citation: Fan, J.; Zhang, Y.; Li, M.; Ji, P.; Tan, H.; Huang, T.; Zhuge, L.; Zhang, X.; Wu, X. A Novel Approach towards the Preparation of Silk-Fibroin-Modified Polyethylene Terephthalate with High Hydrophilicity and Stability. *Coatings* **2024**, *14*, 636. <https://doi.org/10.3390/coatings14050636>

Academic Editor: Csaba Balázs

Received: 16 April 2024

Revised: 11 May 2024

Accepted: 13 May 2024

Published: 17 May 2024



Copyright: © 2024 by the authors. Licensee MDPI, Basel, Switzerland. This article is an open access article distributed under the terms and conditions of the Creative Commons Attribution (CC BY) license (<https://creativecommons.org/licenses/by/4.0/>).

1. Introduction

The utilization of biopolymers such as polylactic acid (PLA), polydimethylsiloxane (PDMS), thermoplastic polyurethane (TPU) and polytetrafluoroethylene (PTFE) in biomedical applications is extensive [1,2]. Polyethylene terephthalate (PET) is the most utilized thermoplastic resin in the polyester series [3–5], exhibits favorable physical-mechanical properties, excellent electrical insulation, cost-effective production, as well as remarkable fatigue resistance, friction resistance, and dimensional stability [6,7], which makes the PET has a highly applicable in the biomedical field in areas such as artificial ligaments, blood vessels, and heart valves [8,9]. However, similar to most polymers, the bio-inert surface of PET is caused by its hydrophobic nature, which limits its potential applications [10]. Therefore, enhancing its hydrophilic property becomes imperative [11].

An effective approach for enhancing the hydrophilic properties of polymer materials involves incorporating biomolecules onto their surfaces. Silk fibroin (SF) is a natural macromolecular protein, typically obtained through the process of silk degumming, constituting

approximately 70%–80% of the total silk mass [12]. It possesses a molecular weight ranging from 3.06×10^5 to 3.7×10^5 and exhibits insolubility in water or ethanol solution. The secondary structure of SF can be classified into a random coil, α -helix, and β -sheet, with the latter being the most stable due to optimal intermolecular interactions and the lowest energy consumption. Due to its distinctive structure, SF shows remarkable characteristics, such as good mechanical properties [13], tunable biodegradability [14,15], and acceptable immunogenicity [16–18]. Additionally, SF can be fabricated into various structures like films [19,20], sponges [21,22], hydrogels [23,24], scaffolds [25,26], and coatings due to its good processability. The SF coatings can improve the chemical activity of substrate materials with minimal immunogenicity [27]. Consequently, immobilizing SF onto PET film presents an avenue for the preparation of SF-modified PET (PET-SF) composites that exhibit enhanced hydrophilicity.

Several techniques are available for immobilizing SF onto the surface of PET. The most widely used technique is solution dip-coating. In this method, the inert surface of PET presents a challenge for direct SF grafting, necessitating its surface activation through techniques such as plasma treatment [28–30], UV irradiation [31], chemical hydrolysis [32,33] or nitration and reduction [34,35]. Following surface activation, SF can be immobilized by immersing the PET substrate in the SF solution. Zhou et al. [36] introduced reactive $-\text{NH}_2$ groups to the surface of PET using the nitration and reduction method, and they modified SF using epoxy chloropropane to introduce active epoxy groups, which enabled SF to be grafted onto the PET surface. The adsorption bands of Fourier transform infrared spectroscopy at 1653 and 1543 cm^{-1} showed a successful introduction of SF. However, it also indicated that the secondary structure of introduced SF was mainly a random coil with an instability in its structure. Ai et al. [37] immobilized SF onto the surface of PET via the EDC/NHS crosslinking method. The results suggested a high concentration of SF, but the improvement in hydrophilicity of PET-SF was limited. The solution dip-coating method can form a relatively high SF concentration but in a low structure stability of SF and limited improvement in hydrophilicity.

An alternative approach is plasma-assisted deposition, which enables the formation of biomacromolecule films on various substrates with different shapes [38]. Moreover, the deposition process occurs at room temperature and atmospheric pressure without using specialized vacuum or heating equipment. In the context of biomacromolecule grafting applications, plasma-assisted deposition typically involves injecting a biomacromolecule aerosol solution into the atmospheric pressure plasma jet (APPJ). This process facilitates simultaneous surface activation of the substrate material and grafting of the biomacromolecule. While SF is immobilized onto the PET surface using atmospheric pressure plasma-assisted deposition technology, SF can be influenced by plasma, leading to the transformation of its secondary structure from a random coil to a β -sheet. Additionally, the presence of argon (Ar) in the deposition area creates an inert atmosphere that facilitates further dehydration of SF and promotes the formation of β -sheet structure. Consequently, atmospheric pressure plasma-assisted deposition enhances the stability of grafted SF while also improving the hydrophilicity of the modified material through surface etching and activation. Arkhangelskiy et al. [39] deposited SF on different materials using APPJ with an SF aerosol solution as the feed gas. The results confirmed the successful immobilization of SF, showing high β -sheet concentration (32 to 38%) and low content of random coil (17 to 18%) due to the effect of plasma. However, the adhesion strength between SF and the surface of polymer materials was relatively low. Therefore, plasma-assisted deposition can address the issues of low structure stability of SF and improve hydrophilicity of modified materials, whereas the SF exhibits relatively lower adhesion to the surface of substrate materials than that achieved through solution dip-coating.

Undoubtedly, the challenge in preparing PET-SF for biomaterial applications resides in the concurrent attainment of several crucial objectives: achieving high surface hydrophilicity, ensuring the structural stability of grafted SF, and promoting strong adhesion strength between SF and PET substrate.

Therefore, this work proposes a novel method for preparing PET-SF with enhanced hydrophilicity, high structure stability and strong adhesion strength between SF and the substrate through two continuous processes: dipping PET film in an SF solution followed by carrying out plasma-assisted deposition using an SF aerosol. Meanwhile, the structure and properties of the PET-SF film prepared by the following three methods were investigated by scanning electron microscopy (SEM), attenuated total reflectance—Fourier-transform infrared spectroscopy (ATR-FTIR), water contact angle (WCA), and X-ray photoelectron spectroscopy (XPS): (1) solution dip-coating; (2) plasma-assisted deposition; and (3) the two-step method. The dipping time and plasma-assisted deposition time in the two-step method were also investigated to gain an optimized procedure for preparing the PET-SF film.

2. Materials and Methods

2.1. Preparation of Silk-Fibroin Solution

The raw silk (100 g) was boiled in an aqueous solution (5 L) containing Na_2CO_3 (2 g) and NaHCO_3 (6 g) for 30 min. Subsequently, the silk was washed with deionized water to remove the sericin from its surface. The degummed silk fibers were dissolved in 9.3 M LiBr at 65 °C using a bath ratio of 1:10 for 1 h to obtain the silk solution. After cooling, the solution was transferred into a dialysis membrane with a molecular weight cut-off of 9–14 kDa and dialyzed with deionized water for 3 days. It was then filtered, centrifuged, and stored in a refrigerator at 4 °C [40].

2.2. Silk Fibroin Immobilization

The PET films (1.5 cm × 1.5 cm × 0.175 mm) were subjected to ultrasonic cleaning in ethanol solution and deionized water for 20 min, respectively. Then, PET films were pretreated under APPJ using Ar as the working gas for 2 min to activate their surfaces. The PET-SF films were prepared using three different methods:

- (1) Solution dip-coating: The pretreated PET films were then immersed in an SF solution and reacted for 12 h at 4 °C [29], referred to as C-PET-SF;
- (2) Plasma-assisted deposition: The pretreated PET films were exposed to APPJ using SF aerosol as the feed gas for 10 min, referred to as P-PET-SF;
- (3) The two-step method: The pretreated PET films were immersed in an SF solution for 6 h at 4 °C and finally subjected to APPJ using SF aerosol as the feed gas for 3 min, referred to as PC-PET-SF.

The diagram of the APPJ device used is shown in Figure 1, where the SF aerosol could be prepared using an ultrasonic nebulizer (positioned in the lower left corner of the figure) and injected into the plasma discharge tube. Subsequently, the aerosol is mixed with the argon plasma and finally deposited on PET films. It is worth noting that when the device does not inject SF aerosol, it functions solely as an Ar APPJ, thereby facilitating surface activation of the material. However, upon turning on the ultrasonic nebulizer and introducing SF aerosol as the feed gas, plasma-assisted deposition of SF can be achieved. The ultrasonic nebulizer employed in the experiment is capable of generating nebulized droplets with a particle size ranging from 1 to 5 μm , exhibiting a nebulization rate of approximately 2 mL/min. The discharge voltage in this experiment exhibited a peak-to-peak value of 20 kV, with the frequency measured at 18 kHz and the Ar flow rate maintained at 3 slm.

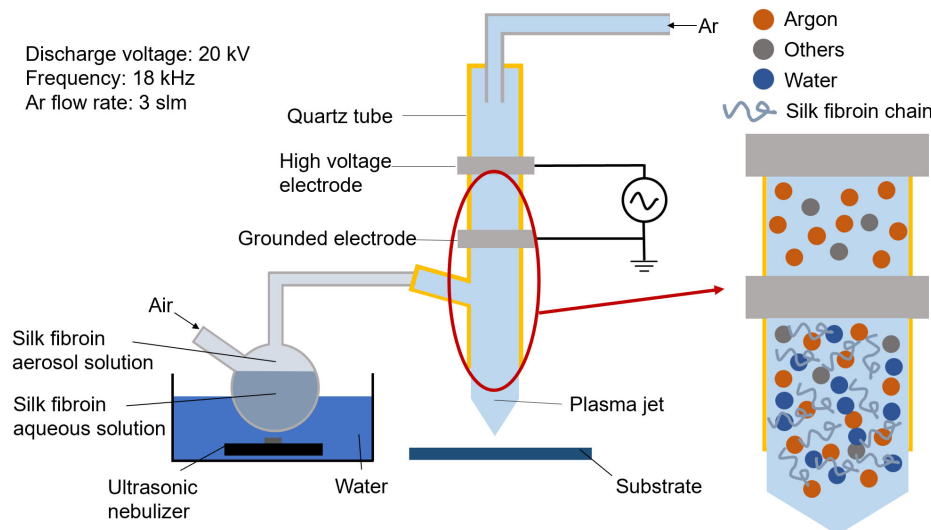


Figure 1. Schematic image of the plasma-assisted deposition system.

2.3. Characterization

The surface morphology of PET-SF films was observed using SEM (SU8100, Hitachi, Tokyo, Japan). Samples were coated with platinum by an ion-sputter coater before the imaging. The structure of the films was studied by ATR-FTIR (VERTEX 70, Bruker, Karlsruhe, Germany). The scanning range was $4000\text{--}650\text{ cm}^{-1}$, the resolution was 4 cm^{-1} , and the number of scans was 32. The surface elemental composition and chemical bonding states were analyzed by XPS (ESCALAB 250XI, Thermo Fisher Scientific, Waltham, MA, USA). The WCA of the samples was measured by a contact angle meter (JC2000DM, POWERREACH, Beijing, China) to estimate the hydrophilicity and hydrophobicity, and measurements were repeated three times for each sample. The alpha-step profiler (Alpha-Step D300, KLA, Milpitas, CA, USA) was employed to measure the step of grafted SF films with the scanning line length of 2 mm and stylus force of 1 mg.

3. Results and Discussion

3.1. PET-SF Films Prepared Using Three Different Methods

The SEM was conducted to investigate the changes in surface morphology of the PET films before and after modification. Figure 2a–d illustrates that the surface of C-PET-SF exhibited relatively smooth, whereas the surfaces of P-PET-SF and PC-PET-SF displayed significant roughness. This phenomenon can be attributed to the active substances in the plasma etching on the substrate surfaces, resulting in an enhancement of surface roughness [41].

The ATR-FTIR spectra in Figure 2e demonstrated the successful introduction of SF onto PET surfaces through all three modification methods, as evidenced by the prominent absorption peak at 3284 cm^{-1} corresponding to the N-H single bond of the SF [42]. Additionally, it can be observed that the characteristic peak of PET substrate at 1713 cm^{-1} in the P-PET-SF spectral line remained prominent, indicating a low and insufficient density of SF grafted through the plasma-assisted deposition method. However, the characteristic peaks of PET substrate in C-PET-SF and PC-PET-SF spectral lines exhibited minimal intensity, indicating that the grafting amount and density of SF on the modified PET surface through the solution dip-coating and the two-step methods is sufficient to effectively dilute the infrared signal of the PET substrate. The amide I region of SF exhibited adsorption bands at 1648 cm^{-1} (indicative of a random coil structure) and 1624 cm^{-1} (indicative of a β -sheet structure) [40]. Comparative analysis revealed that P-PET-SF and PC-PET-SF exhibited higher quantities of β -sheet structures compared to C-PET-SF, suggesting that SF immobilized via plasma-assisted deposition or the two-step method could achieve a

more stable secondary structure, primarily attributable to the dehydration process and the influence of plasma [43].

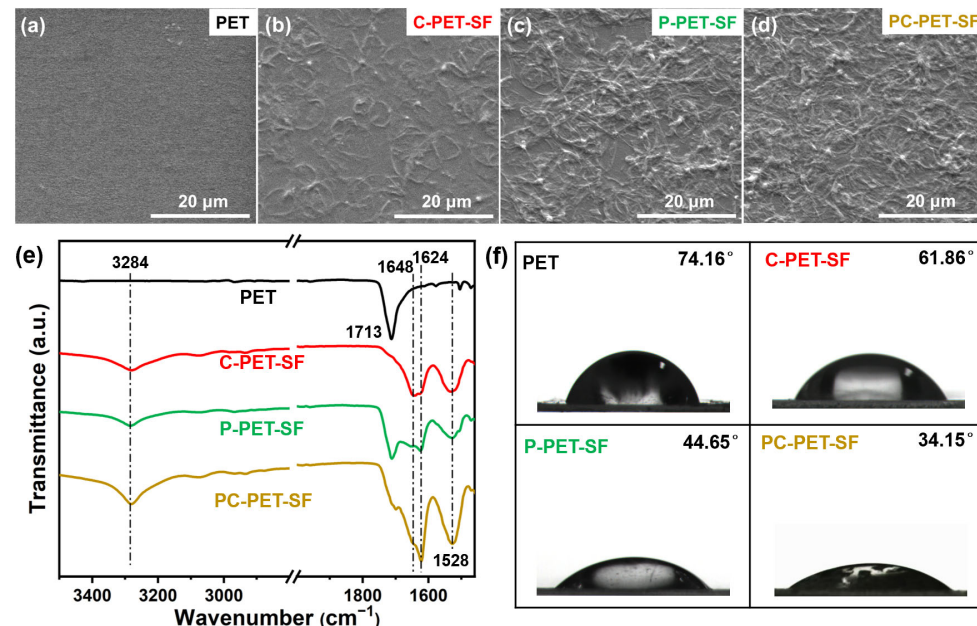


Figure 2. SEM morphologies of (a) PET; (b) C-PET-SF; (c) P-PET-SF; (d) PC-PET-SF; (e) ATR-FTIR spectra, and (f) WCA of PET and PET-SF films.

The immobilization of SF caused varying changes in the WCA of PET, as shown in Figure 2f. Upon solution dip-coating with SF, the WCA of PET decreased from 74.16° to 61.86° , while plasma-assisted deposition further reduced it to 44.65° . However, employing a two-step method resulted in a significant reduction in the WCA of modified PET to 34.15° and achieved optimal hydrophilicity effect. This can be attributed to the improved surface roughness of the material, as increasing surface roughness is known to reduce WCA for hydrophilic materials ($\text{WCA} < 90^\circ$) [44].

In addition to surface roughness, the hydrophilicity of the material is also influenced by the presence of hydrophilic functional groups on its surface. The chemical structure of the PET-SF surfaces was further examined using XPS measurements. As shown in Figure 3a, upon immobilization of SF, a prominent peak corresponding to N1s (BE, 399 eV) was observed, providing additional evidence for successful SF introduction. The chemical composition was determined from high-resolution scan spectra and presented in Figure 3b. Firstly, the N/C ratio in this study is directly correlated with the concentration of SF grafted onto the surface of PET. The calculated N/C ratios for C-PET-SF, P-PET-SF, and PC-PET-SF were 0.29, 0.27, and 0.30, respectively, indicating that the two-step method can achieve the highest SF grafting amount. Additionally, the O/C ratio is closely related to the concentration of oxygen-containing functional groups on the surface of the material. Comparatively, PC-PET-SF exhibited the highest O/C ratio of 0.38, indicating that PET-SF prepared through the two-step method possessed a higher concentration of oxygen-containing functional groups. The high-resolution C1s spectra of different film surfaces are presented in Figure 3c–f, allowing for the calculation of functional group percentages. For the untreated PET film, the spectrum was curve-fitted into three peaks at binding energies of 284.6–285 eV (C–C/H), 286.4–287 eV (C–O), and 288.5–289.6 eV (O=C–O–H/C) with corresponding percentages of 68.07%, 17.66%, and 14.27% respectively. After further immobilization of SF, the peaks shifted to 284.6–285 eV (C–C/H), 285.5–286.5 eV (C–N), and 287.4–288.4 eV (N–C=O) [45]. It can be calculated that the N–C=O percentages for C-PET-SF, P-PET-SF, and PC-PET-SF were determined as 26.57%, 27.24%, and 27.30% respectively,

indicating that the two-step method can provide PET-SF with the highest concentration of hydrophilic functional groups capable of enhancing material surface hydrophilicity.

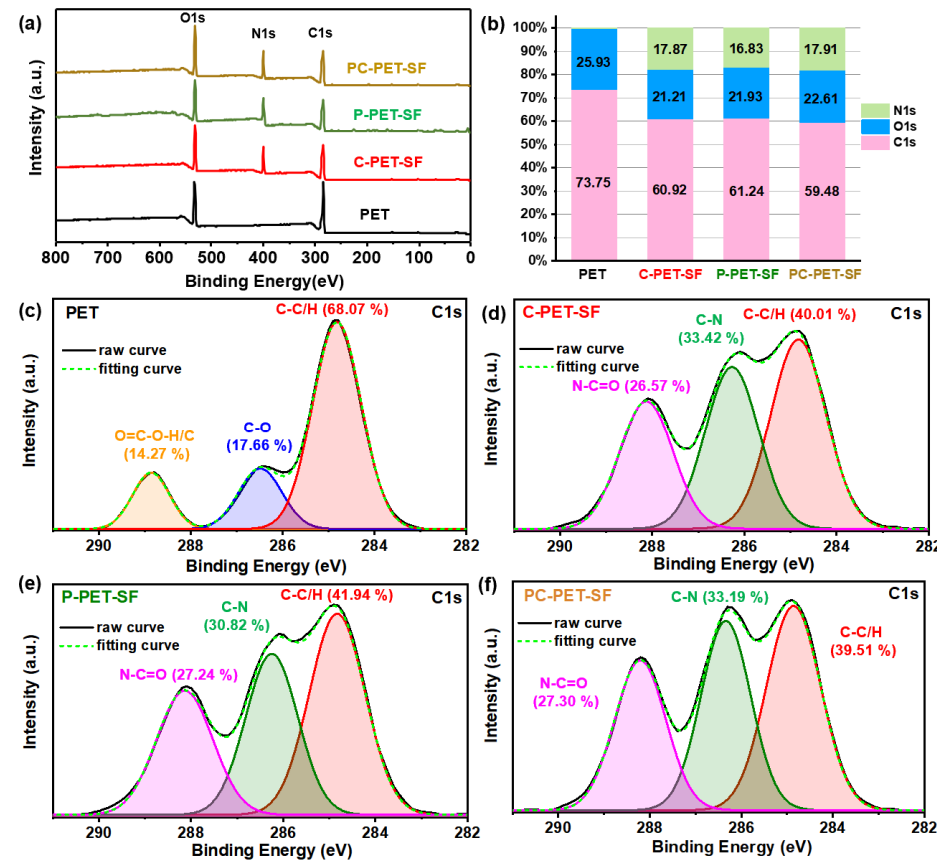


Figure 3. (a) XPS spectra of PET, C-PET-SF, P-PET-SF and PC-PET-SF; (b) chemical composition of PET-SF, and deconvolution of C1s of (c) PET; (d) C-PET-SF; (e) P-PET-SF and (f) PC-PET-SF.

The aging effect of PET-SF films was evaluated by storing them in a desiccator at ambient temperature for 20 days. The WCA of the modified PET films was re-measured and depicted in Figure 4a. After 20 days of storage, the WCA of three samples was almost unchanged. These results suggested that all three preparation methods provide PET-SF with remarkable resistance against aging.

In order to compare the adhesion strength of SF on PET substrates prepared by three different methods, the modified PET samples were subjected to rinsing with deionized water on a shaking table at 37 °C for 10 days. The post-dissolution ATR-FTIR spectra of PET-SF are presented in Figure 4b–d. The intensity of 1648 cm⁻¹ in the C-PET-SF spectral line had a significant increase after being rinsed with deionized water for 10 days, suggesting that SF immobilized by dip-coating easily transferred from a more stable β -sheet structure to a random coil structure in aqueous environment (Figure 4b). The peaks at 3284 cm⁻¹, 1648 cm⁻¹, and 1624 cm⁻¹ in the P-PET-SF spectral line disappeared after the rinsing process, indicating weak adhesion between SF and PET film, resulting in SF peeling off from PET in aqueous environment (Figure 4c). The spectrum of PC-PET-SF film did not change significantly after being rinsed with deionized water (Figure 4d). The results suggested that the adhesion strength between SF and the surface of the PET substrate is significantly enhanced when prepared using solution dip-coating or the two-step method. In contrast, it is comparatively weaker when solely prepared through plasma-assisted deposition. Furthermore, the structure of SF immobilized via dip-coating exhibits instability. This discrepancy may be attributed to prolonged etching during plasma-assisted deposition, resulting in a rougher morphology on the surface of the PET substrate and thus forming

delamination regions. When these samples are rinsed with deionized water, it is possible for water molecules to penetrate through these delaminated areas, thereby weakening the adhesion strength between SF and the PET surface [46].

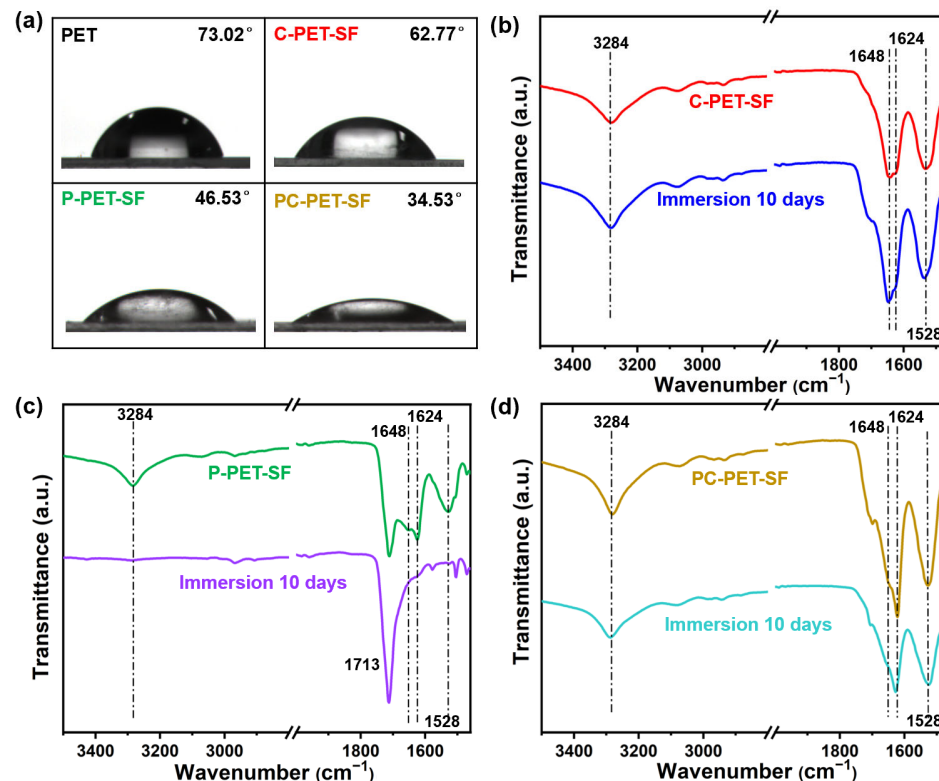


Figure 4. (a) WCA of PET and PET-SF films after storage in air for 20 days; (b–d) ATR-FTIR spectra of C-PET-SF, P-PET-SF and PC-PET-SF before and after being rinsed in deionized water for 10 days at 37 °C.

3.2. Influence of Treatment Time in the Two-Step Method

The effect of dipping time and plasma-assisted deposition time on the structure and properties of PET-SF films prepared by the two-step method was employed. The specific experimental parameters were as follows:

1. Fixed plasma deposition time of 3 min while varying dipping times at 1 h, 2 h, 3 h, 4 h, 6 h, 8 h, 12 h, and 24 h;
- (4) Fixed dipping time of 6 h while varying plasma deposition times at intervals of 30 s, 1 min, 2 min, 3 min, 4 min, 6 min, 8 min, and 12 min.

Figure 5a presents the ATR-FTIR spectra of grafted SF with varying dipping times. Initially, based on the characteristic peak positions of amide I (1624 cm^{-1} representing β -sheet) and amide II (1528 cm^{-1} representing β -sheet), it can be observed that the secondary structure of SF primarily consisted of β -sheet, which remained unaffected by the dipping time. This indicated that the dipping time in the two-step method does not influence the structure stability of grafted SF within a specific thickness range. This phenomenon can be attributed to the uniform and dense SF film achieved within a 3-min plasma-assisted deposition, effectively masking infrared signals originating from underlying layers of SF grafted through dip-coating. Consequently, altering only the dipping time while maintaining a constant deposition time does not influence the SF secondary structure detected via infrared spectroscopy. Furthermore, increasing dipping time weakened the infrared signal of the PET substrate at 1713 cm^{-1} ; after reaching 6 h, this signal became extremely weak and remained relatively stable thereafter. These findings suggested that

a longer dipping time results in a higher grafting amount of SF, and after 6 h, there is a sufficient grafting amount of SF to dilute the infrared signal of the PET substrate.

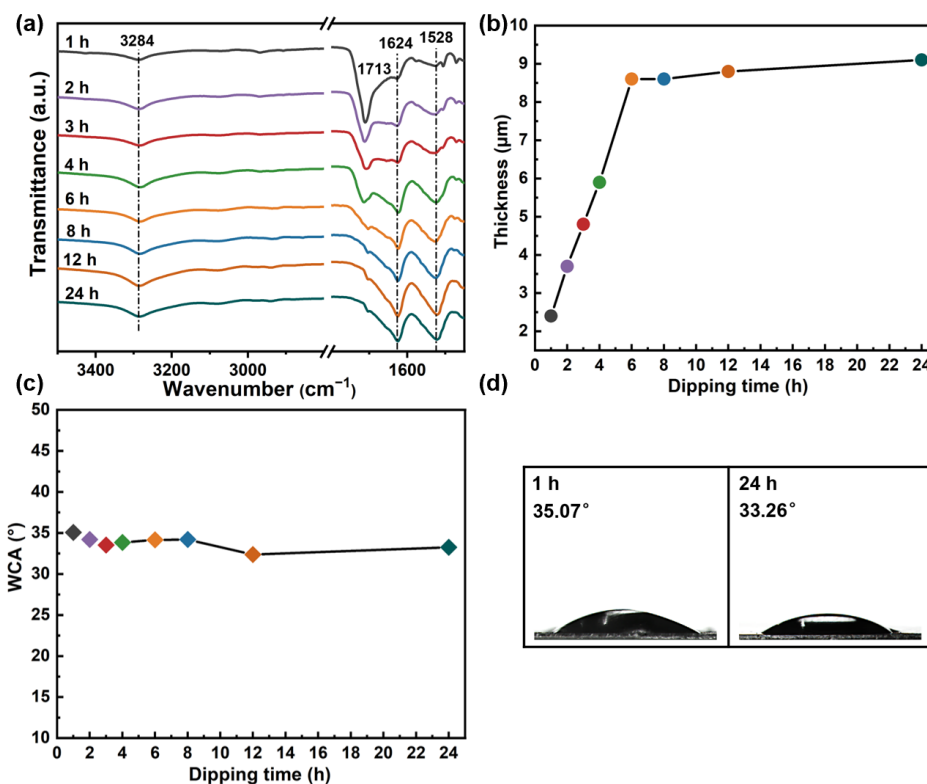


Figure 5. (a) ATR-FTIR spectra of grafted SF with varying dipping times; (b) thickness of grafted SF with varying dipping times; (c) WCA of modified PET with varying dipping times; (d) WCA at dipping time of 1 h and 24 h.

The thickness of grafted SF on the PET surface as a function of dipping time is illustrated in Figure 5b. It can be observed that the thickness of SF increased with increasing dipping time, reaching a maximum value of 8.6 μm at 6 h and keeping a relatively stable value after 6 h. Therefore, an ideal thickness of SF can be obtained when the dipping time is more than 6 h. Figure 5c,d depict the variation in WCA as a function of dipping time. It can be observed that the dipping time has no significant effect on the hydrophilicity of PET-SF since the WCA values remained relatively constant within the range of 32.36° to 35.07°.

The ATR-FTIR spectra of PET-SF films obtained by varying the plasma deposition time are presented in Figure 6a. Initially, the PET characteristic peak intensity at 1713 cm^{-1} was observed to be extremely weak for deposition times ranging from 1 to 4 min. However, as the deposition time increased to 6 min, there was a corresponding increase in the intensity of the PET characteristic peak. This phenomenon can be attributed to the enhanced etching strength of plasma on the grafted SF film and increased inhomogeneity in deposited SF at longer deposition times, leading to partial exposure of the PET substrate. The secondary structure of SF was subsequently investigated. Based on the characteristic peaks of amide I (random coil at 1648 cm^{-1} , β -sheet at 1624 cm^{-1}) and amide II (random coil at 1541 cm^{-1} , β -sheet at 1528 cm^{-1}), it can be observed that with an increase in deposition time from 30 s, there was a continuous increase in the proportion of β -sheet in SF until reaching its maximum value at 3 min. At this point, the SF secondary structure primarily comprised β -sheet with minimal presence of random coil. Further extension of the deposition time resulted in an increase in random coil content while concurrently reducing the proportion of β -sheet until the random coil became dominant after 8 min. Consequently, it can be concluded that a relatively stable secondary structure of SF can be achieved when deposited for 2–3 min. The probable reason is that, as mentioned in the previous section, the secondary

structure of SF immobilized through solution dip-coating predominantly consists of the random coil, while SF immobilized via plasma-assisted deposition primarily comprises a β -sheet. When the deposition time was extended to 4 min, there was an enhancement in plasma etching, thereby exposing the underlying SF grafted by solution dip-coating.

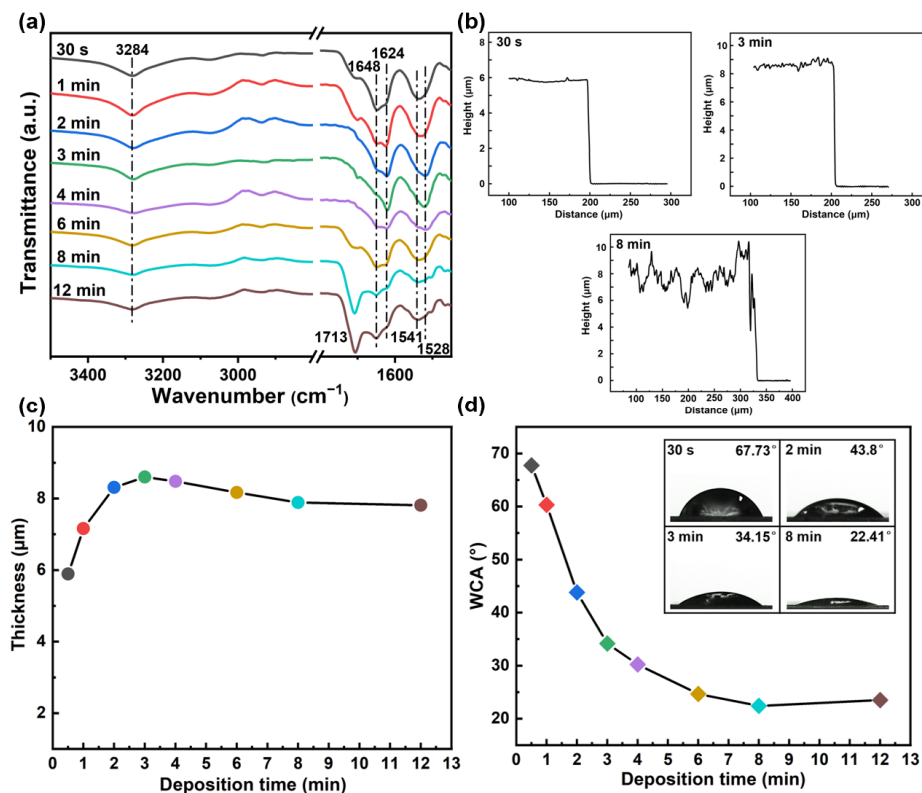


Figure 6. (a) ATR-FTIR spectra of grafted SF with varying deposition times; (b) steps at deposition times of 30 s, 3 min and 8 min; (c) thickness of grafted SF with varying deposition times; (d) WCA of modified PET with varying deposition times.

The thickness of SF films on PET as a function of deposition time was measured by the step profiler, which is illustrated in Figure 6c. The thickness of the SF film was observed to progressively increase with prolonged deposition time, ultimately reaching a maximum value of 8.6 μm after 3 min. However, further prolonging the deposition time resulted in a slight reduction in SF thickness. Figure 6b displays the steps of SF measured at plasma deposition times of 30 s, 3 min, and 8 min. It can be seen that when the deposition time was only 30 s, the surface of the grafted SF appeared relatively flat. With an increase in deposition time to 3 min, surface roughness improved but remained relatively uniform overall. However, when extending the deposition time to 8 min, significant roughness and non-uniform distribution were observed on the SF film surface due to enhanced plasma etching effects. This finding is consistent with the results of the infrared spectrum test which helps explain why deposition times longer than 3 min no longer led to an increased thickness for immobilized SF films.

The WCA of PET-SF films as a function of deposition time is illustrated in Figure 6d, indicating an initial rapid decline followed by a slower decrease and eventual stabilization. Specifically, at a deposition time of 30 s, the WCA was 67.73° , which closely resembles that of the untreated PET film. Subsequently, the WCA decreased rapidly until reaching 34.15° within 3 min, achieving an ideal hydrophilic effect. At 8 min, the WCA reached a lower value of 22.41° and was unchanged too much, with a further increase in deposition time. Consequently, the hydrophilicity of PET-SF film achieved satisfactory levels after a deposition time of 3 min and reached its optimum at 8 min using the two-step method.

4. Conclusions

An effective approach was developed to prepare high hydrophilicity and stability silk-fibroin-modified PET film through two consecutive processes: dipping PET film in an SF solution and subsequently carrying out plasma-assisted deposition in an SF aerosol. PET-SF prepared using the two-step method exhibited superior structural stability, stronger adhesion strength, and higher surface hydrophilicity compared to the solution dip-coating and plasma-assisted deposition methods.

- (1) The dipping process resulted in a strong adhesion strength between SF and the PET substrate. The plasma contributed to converting the SF secondary structure from a random coil to a more stable β -sheet structure and forming hydrophilic functional groups.
- (2) The dipping time for 6 h and the deposition time for 3 min resulted in a maximum SF grafting amount with a highly stable structure.
- (3) The modified PET exhibited satisfactory hydrophilicity when the deposition time was more than 3 min and showed the most hydrophilicity surface at 8 min.

Author Contributions: Conceptualization, J.F.; methodology, J.F.; software, J.F.; validation, J.F.; formal analysis, J.F.; investigation, J.F.; resources, J.F., Y.Z., X.Z. and L.Z.; data curation, J.F.; writing—original draft preparation, J.F.; writing—review and editing, X.Z. and Y.Z.; visualization, J.F.; supervision, X.Z., M.L., P.J., H.T. and T.H.; project administration, X.Z. and X.W.; funding acquisition, X.W. All authors have read and agreed to the published version of the manuscript.

Funding: This research was funded by the National Natural Science Foundation of China, No. 11975163, 12175160, 12305284; the National Key R&D Program of China, No. 2022YFE03050001; a Project Funded by the Priority Academic Program Development of Jiangsu Higher Education Institutions (PAPD), and Jiangsu Funding Program for Excellent Postdoctoral.

Institutional Review Board Statement: Not applicable.

Informed Consent Statement: Not applicable.

Data Availability Statement: Data are contained within the article.

Conflicts of Interest: The authors declare no conflicts of interest.

References

1. Drobotă, M.; Ursache, S.; Aflori, M. Surface functionalities of polymers for biomaterial applications. *Polymers* **2022**, *14*, 2307. [[CrossRef](#)] [[PubMed](#)]
2. Hoque, M.E.; Rayhan, A.M.; Shaily, S.I. Natural fiber-based green composites: Processing, properties and biomedical applications. *Appl. Sci. Eng.* **2021**, *14*, 689. [[CrossRef](#)]
3. Afonso, E.; Martinez-Gomez, A.; Huerta, A.; Tiemblo, P.; Garcia, N. Facile preparation of hydrophobic PET surfaces by solvent induced crystallization. *Coatings* **2022**, *12*, 137. [[CrossRef](#)]
4. Wu, J.; Wu, K.; Chen, J.; Song, C.; Jia, P.; Li, X. Influence of air addition on surface modification of polyethylene terephthalate treated by an atmospheric pressure argon plasma brush. *Plasma Sci. Technol.* **2021**, *23*, 085504. [[CrossRef](#)]
5. El-Saftawy, A.A.; Elfalaky, A.; Ragheb, M.S.; Zakhary, S.G. Electron beam induced surface modifications of PET film. *Radiat. Phys. Chem.* **2014**, *102*, 96–102. [[CrossRef](#)]
6. Mui, T.S.M.; Mota, R.P.; Quade, A.; de Oliveira Hein, L.R.; Kostov, K.G. Uniform surface modification of polyethylene terephthalate (PET) by atmospheric pressure plasma jet with a horn-like nozzle. *Surf. Coat. Technol.* **2018**, *352*, 338–347. [[CrossRef](#)]
7. Caykara, T.; Silva, J.; Fernandes, S.; Braga, A.; Rodrigues, J.; Rodrigues, L.R.; Silva, C. Modification of PET surfaces with gum Arabic towards its bacterial anti-adhesiveness using an experimental factorial design approach. *Mater. Today Commun.* **2021**, *28*, 102684. [[CrossRef](#)]
8. Mao, Y.; Li, Q.; Wu, C. Surface modification of PET fiber with hybrid coating and its effect on the properties of PP composites. *Polymers* **2019**, *11*, 1726. [[CrossRef](#)]
9. Lai, J.; Sunderland, B.; Xue, J.; Yan, S.; Zhao, W.; Folkard, M.; Michael, B.D.; Wang, Y. Study on hydrophilicity of polymer surfaces improved by plasma treatment. *Appl. Surf. Sci.* **2006**, *252*, 3375–3379. [[CrossRef](#)]
10. Klein, M.O.; Bijelic, A.; Toyoshima, T.; Gotz, H.; von Koppenfels, R.L.; Al-Nawas, B.; Duschner, H. Long-term response of osteogenic cells on micron and submicron-scale-structured hydrophilic titanium surfaces: Sequence of cell proliferation and cell differentiation. *Clin. Oral Implant. Res.* **2010**, *21*, 642–649. [[CrossRef](#)]
11. Ma, Z.; Mao, Z.; Gao, C. Surface modification and property analysis of biomedical polymers used for tissue engineering. *Colloids Surf. B* **2007**, *60*, 137–157. [[CrossRef](#)] [[PubMed](#)]

12. Popescu, S.; Zarif, M.E.; Dumitriu, C.; Ungureanu, C.; Pirvu, C. Silk fibroin-based hybrid nanostructured coatings for titanium implantable surfaces modification. *Coatings* **2020**, *10*, 518. [[CrossRef](#)]
13. Porter, D.; Vollrath, F. Silk as a biomimetic ideal for structural polymers. *Adv. Mater.* **2009**, *21*, 487–492. [[CrossRef](#)]
14. Ma, D.; Wang, Y.; Dai, W. Silk fibroin-based biomaterials for musculoskeletal tissue engineering. *Mater. Sci. Eng. C* **2018**, *89*, 456–469. [[CrossRef](#)] [[PubMed](#)]
15. Tomeh, M.A.; Hadianamrei, R.; Zhao, X. Silk fibroin as a functional biomaterial for drug and gene delivery. *Pharmaceutics* **2019**, *11*, 494. [[CrossRef](#)] [[PubMed](#)]
16. Meinel, L.; Fajardo, R.; Hofmann, S.; Langer, R.; Chen, J.; Snyder, B. Silk implants for the healing of critical size bone defects. *Bone* **2005**, *37*, 688–698. [[CrossRef](#)] [[PubMed](#)]
17. Altman, G.H.; Horan, R.L.; Lu, H.H.; Moreau, J.; Martin, I.; Richmond, J.C.; Kaplan, D.L. Silk matrix for tissue engineered anterior cruciate ligaments. *Biomaterials* **2002**, *23*, 4131–4141. [[CrossRef](#)]
18. Unger, R.E.; Wolf, M.; Peters, K.; Motta, A.; Migliaresi, C.; Kirkpatrick, C.J. Growth of human cells on a non-woven silk fibroin net: A potential for use in tissue engineering. *Biomaterials* **2004**, *25*, 1069–1075. [[CrossRef](#)]
19. Ming, J.; Liu, Z.; Bie, S.; Zhang, F.; Zuo, B. Novel silk fibroin films prepared by formic acid/hydroxyapatite dissolution method. *Mater. Sci. Eng. C* **2014**, *37*, 48–53. [[CrossRef](#)]
20. Youn, Y.H.; Pradhan, S.; Da Silva, L.P.; Kwon, I.K.; Kundu, S.C.; Reis, R.L.; Yadavalli, V.K.; Correlo, V.M. Micropatterned silk-fibroin/eumelanin composite films for bioelectronic applications. *ACS Biomater. Sci. Eng.* **2021**, *7*, 2466–2474. [[CrossRef](#)]
21. Liu, J.; Xie, X.; Wang, T.; Chen, H.; Fu, Y.; Cheng, X.; Wu, J.; Li, G.; Liu, C.; Liimatainen, H.; et al. Promotion of wound healing using nanoporous silk fibroin sponges. *ACS Appl. Mater. Interfaces* **2023**, *15*, 12696–12707. [[CrossRef](#)] [[PubMed](#)]
22. Sionkowska, A.; Michalska, M.; Walczak, M. Preparation and characterization of silk fibroin/collagen sponge with nanohydroxyapatite. *Mol. Cryst. Liq. Cryst.* **2016**, *640*, 106–112. [[CrossRef](#)]
23. Chouhan, D.; Lohe, T.; Samudrala, P.K.; Mandal, B.B. In Situ forming injectable silk fibroin hydrogel promotes skin regeneration in full thickness burn wounds. *Adv. Healthc. Mater.* **2018**, *7*, 1801092. [[CrossRef](#)]
24. He, S.; Shi, D.; Han, Z.; Dong, Z.; Xie, Y.; Zhang, F.; Zeng, W.X.; Yi, Q. Heparinized silk fibroin hydrogels loading FGF1 promote the wound healing in rats with full-thickness skin excision. *BioMed. Eng. OnLine* **2019**, *18*, 97. [[CrossRef](#)] [[PubMed](#)]
25. Li, Z.; Ji, S.; Wang, Y.; Shen, X.; Liang, H. Silk fibroin-based scaffolds for tissue engineering. *Front. Mater. Sci.* **2013**, *7*, 237–247. [[CrossRef](#)] [[PubMed](#)]
26. Kuboyama, N.; Kiba, H.; Arai, K.; Uchida, R.; Tanimoto, Y.; Bhawal, U.K.; Abiko, Y.; Miyamoto, S.; Knight, D.; Asakura, T.; et al. Silk fibroin-based scaffolds for bone regeneration. *J. Biomed. Mater. Res. Part B* **2013**, *101B*, 295–302. [[CrossRef](#)]
27. Hu, J.; Jiang, Z.; Zhang, J.; Yang, G. Application of silk fibroin coatings for biomaterial surface modification: A silk road for biomedicine. *J. Zhejiang Univ. Sci. B* **2023**, *24*, 943–956. [[CrossRef](#)] [[PubMed](#)]
28. Tkavc, T.; Petrinic, I.; Luxbacher, T.; Vesel, A.; Ristic, T.; Zemljic, L.F. Influence of O₂ and CO₂ plasma treatment on the deposition of chitosan onto polyethylene terephthalate (PET) surfaces. *Int. J. Adhes. Adhes.* **2014**, *48*, 168–176. [[CrossRef](#)]
29. Liang, M.; Yao, J.; Chen, X.; Huang, L.; Shao, Z. Silk fibroin immobilization on poly(ethylene terephthalate) films: Comparison of two surface modification methods and their effect on mesenchymal stem cells culture. *Mater. Sci. Eng. C* **2013**, *33*, 1409–1416. [[CrossRef](#)]
30. Poletti, G.; Orsini, F.; Raffaele-Addamo, A.; Riccardi, C.; Sellì, E. Cold plasma treatment of PET fabrics: AFM surface morphology characterization. *Appl. Surf. Sci.* **2003**, *219*, 311–316. [[CrossRef](#)]
31. Zhu, Z.; Kelley, M. Poly(ethylene terephthalate) surface modification by deep UV (172 nm) irradiation. *Appl. Surf. Sci.* **2004**, *236*, 416–425. [[CrossRef](#)]
32. Eberl, A.; Heumann, S.; Brückner, T.; Araujo, R.; Cavaco-Paulo, A.; Kaufmann, F.; Kroutil, W.; Guebitz, G.M. Enzymatic surface hydrolysis of poly(ethylene terephthalate) and bis(benzoyloxyethyl) terephthalate by lipase and cutinase in the presence of surface active molecules. *J. Biotechnol.* **2009**, *143*, 207–212. [[CrossRef](#)] [[PubMed](#)]
33. Wei, Z.; Gu, Z. A study of one-bath alkali-amine hydrolysis and silk fibroin finishing of polyester microfiber crepe fabric. *J. Appl. Polym. Sci.* **2001**, *81*, 1467–1473. [[CrossRef](#)]
34. Gupta, B.; Plummer, C.; Bisson, I.; Frey, P.; Hilborn, J. Plasma-induced graft polymerization of acrylic acid onto poly(ethylene terephthalate) films: Characterization and human smooth muscle cell growth on grafted films. *Biomaterials* **2002**, *23*, 863–871. [[CrossRef](#)]
35. Kim, Y.J.; Kang, I.K.; Huh, M.W.; Yoon, S.C. Surface characterization and in vitro blood compatibility of poly(ethylene terephthalate) immobilized with insulin and/or heparin using plasma glow discharge. *Biomaterials* **2000**, *21*, 121–130. [[CrossRef](#)] [[PubMed](#)]
36. Zhou, J.; Zheng, D.; Zhang, F.; Zhang, G. Durable grafting of silkworm pupa protein onto the surface of polyethylene terephthalate fibers. *Mater. Sci. Eng. C* **2016**, *69*, 1290–1296. [[CrossRef](#)]
37. Ai, C.; Cai, J.; Zhu, J.; Zhou, J.; Jiang, J.; Chen, S. Effect of PET graft coated with silk fibroin via EDC/NHS crosslink on graft-bone healing in ACL reconstruction. *RSC Adv.* **2017**, *7*, 51303–51312. [[CrossRef](#)]
38. Carnide, G.; Cacot, L.; Champouret, Y.; Pozsgay, V.; Verdier, T.; Girardeau, A.; Cavarroc, M.; Sarkissian, A.; Mingotaud, A.F.; Vahlas, C.; et al. Direct liquid reactor-injector of nanoparticles: A safer-by-design aerosol injection for nanocomposite thin-film deposition adapted to various plasma-assisted processes. *Coatings* **2023**, *13*, 630. [[CrossRef](#)]

39. Arkhangelskiy, A.; Maniglio, D.; Bucciarelli, A.; Yadavalli, V.K.; Quaranta, A. Plasma-assisted deposition of silk fibroin on different surfaces. *Adv. Mater. Interfaces* **2021**, *8*, 2100324. [[CrossRef](#)]
40. Shi, P.; Zhang, L.; Tian, W.; Li, H.; Wang, Q.; Yi, H.; Yin, Y.; Wang, A.; Ning, P.; Dong, F.; et al. Preparation and anticoagulant activity of functionalised silk fibroin. *Chem. Eng. Sci.* **2019**, *199*, 240–248. [[CrossRef](#)]
41. Jacobs, T.; Morent, R.; Geyter, N.D.; Dubrule, P.; Leys, C. Plasma surface modification of biomedical polymers: Influence on cell-material interaction. *Plasma Chem. Plasma Process.* **2012**, *32*, 1039–1073. [[CrossRef](#)]
42. Kamalha, E.; Zheng, Y.S.; Zeng, Y.C.; Fredrick, M.N. FTIR and WAXD study of regenerated silk fibroin. *Adv. Mater. Res.* **2013**, *677*, 211–215. [[CrossRef](#)]
43. Ling, S.; Qi, Z.; Knight, D.P.; Shao, Z.; Chen, X. Synchrotron FTIR microspectroscopy of single natural silk fibers. *Biomacromolecules* **2011**, *12*, 3344–3349. [[CrossRef](#)] [[PubMed](#)]
44. Adamczyk, A. The influence of organically modified derivatives of silica on the structure and the wetting angle values of silica coatings. *Coatings* **2021**, *11*, 1058. [[CrossRef](#)]
45. Amornsudthiwat, P.; Mongkolnavin, R.; Kanokpanont, S.; Panpranot, J.; Wong, C.S.; Damrongsakkul, S. Improvement of early cell adhesion on Thai silk fibroin surface by low energy plasma. *Colloids Surf. B Biointerfaces* **2013**, *111*, 579–586. [[CrossRef](#)]
46. Arkhangelskiy, A.; Quaranta, A.; Motta, A.; Yang, Y.; Yadavalli, V.K.; Maniglio, D. Atmospheric plasma-assisted deposition and patterning of natural polymers. *Adv. Mater. Interfaces* **2022**, *9*, 2200454. [[CrossRef](#)]

Disclaimer/Publisher's Note: The statements, opinions and data contained in all publications are solely those of the individual author(s) and contributor(s) and not of MDPI and/or the editor(s). MDPI and/or the editor(s) disclaim responsibility for any injury to people or property resulting from any ideas, methods, instructions or products referred to in the content.